Infection, Genetics and Evolution 80 (2020) 104199

Contents lists available at ScienceDirect

Infection, Genetics and Evolution

journal homepage: www.elsevier.com/locate/meegid

Research Paper

Immunoinformatics guided rational design of a next generation multi epitope based peptide (MEBP) vaccine by exploring Zika virus proteome

Farah Shahid, Usman Ali Ashfaq*, Anam Javaid, Hina Khalid

Department of Bioinformatics and Biotechnology, Government College University, Faisalabad, Pakistan

ARTICLE INFO

Keywords:
Multi-epitope vaccine
Immuno-informatics
Adjuvant
Molecular docking

ABSTRACT

Zika virus (ZIKV) is an RNA virus that has spread through mosquito sting. Currently, no vaccine and antiviral medication available so far against ZIKV. Therefore, it has fostered a study to design MEBP vaccine enabling effective prevention against the ZIKV infection. In this study combination of immuno-informatics and molecular docking approach was used to constitute a MEBP vaccine. The ZIKV proteome was used for prediction of B-cell, T-cell (HTL & CTL) and IFN-γ epitopes. After prediction, highly antigenic and overlapping epitopes have been shortlisted which includes 14 CTL and 11 HTL epitopes that have been linked to the final peptide through AAY and GPGPG linkers respectively. An adjuvant at the N-end of the vaccine was added to improve the immunogenicity of the vaccine through the EAAAK linker. The final construct constitutes 435 amino acids after the addition of linkers and adjuvant. The existence of B-cell and IFN-γ epitopes affirms the humoral and cell-mediated immune responses acquired by the construct. Allergenicity, antigenicity and different physiochemical attributes of the vaccine were evaluated to assure its safety and immunogenicity profile. In fact, the construct was antigenic and non-allergenic. Docking was performed among vaccine and TLR-3 to evaluate the binding affinity and the molecular interaction. Finally, the construct was subjected to In silico cloning to confers the authenticity of its expression efficiency. However, the proposed construct need to be validate experimentally to ensure its safety and immunogenic profile.

1. Introduction

ZIKV is an RNA virus with a genome length of 10.7 kb and belongs to the family of Flaviviridae. The enzymes from virus and host cell proteases processes the polyprotein into seven non-structural and three structural proteins. The structural proteins includes Capsid-C, pre-membrane / layer protein – prM / M, and envelope-E that form the infectious particle (Lindenbach and Rice, 2003; Mirza et al., 2016). On the other hand, non-structural proteins consists of NS1-NS5 that participates in formation of replication machinery (Sirohi and Kuhn, 2017). ZIKV is mostly transmitted by the bite of mosquito of the species such as *A. albopictus, A. africanus, and A. aegypti* (Faria et al., 2016). Apart from mosquito bite, direct sexual contact is also considered to be a significant transmission passage for ZIKV in humans. (Faye et al., 2014).

In 1947, ZIKV was early screened in the woodland of Uganda from a rhesus monkey. The forest is known as the Zika forest. After the primary screening of the virus, a few human cases have been reported across Asia and Africa. Antibodies against ZIKV have been observed in many non-human primates, but humans predominantly is considered as its host in the absence of other primates (Buathong et al., 2015). The ZIKV in the amniotic fluid of a pregnant woman resulted in microcephaly in newborn babies (Calvet et al., 2016). The symptoms of the ZIKV include headache, severe fatigue, malaise, arthralgia, non-purulent conjunctivitis, and fever (Ashfaq and Ahmed, 2016; Faye et al., 2014; Foy et al., 2011; Musso et al., 2015).

The first case of ZIKV in human was first reported in Nigeria in 1953, and the virus was confirmed in three sick people (Macnamara, 1954). Despite the recognition that ZIKV infection can cause mild febrile illness, only 13 cases have been reported spontaneously over the next 57 years (Fagbami, 1979; Moore et al., 1975; Olson and Ksiazek, 1981). The outbreak in 2007 on several islands of the Yap State, Federated States of Micronesia, was a big surprise that about 5000 out of a population of 6700 were infected (Duffy et al., 2009).

Since then, outbreaks in French Polynesia in 2013 and 2014 have been estimated to involve 32,000 people who have been assessed as suspected of having a ZIKV infection (Cao-Lormeau et al., 2014; Mallet et al., 2016; Prevention and Control, 2014).

ZIKV was first identified in the Continental United States in March 2015, when a rash outbreak occurred in Bahia, Brazil (Campos et al., 2015; Zanluca et al., 2015). Epidemiological data showed that in

* Corresponding author.
E-mail address: ashfaqua@gcuf.edu.pk (U.A. Ashfaq).

https://doi.org/10.1016/j.meegid.2020.104199
Received 14 November 2019; Received in revised form 13 January 2020; Accepted 17 January 2020
Available online 18 January 2020
1567-1348/ © 2020 Elsevier B.V. All rights reserved.

Salvador, the capital of Bahia, the epidemic began in February and lasted until June 2015 (Cardoso et al., 2015). By October, the virus had spread to at least 14 Brazilian states (WHO, 2015), and by December 2015 the Brazilian Ministry of Health estimated that there were 1.3 million suspected cases. In October 2015, Colombia reported the first infectious ZIKV disease outside Brazil (WHO, 2015) and on March 3, 2016, 51,473 suspected ZIKV cases were reported there. By March 2016, the virus had spread to at least 33 countries and regions in the Americas (Hennessey et al., 2016).

In September 2015, a Brazilian researcher observed an increase in the number of babies born with microcephaly in the same area where ZIKV was first reported (Schuler-Faccini, 2016). By mid-February 2016, over 4300 cases of microcephaly were reported, but this number may have increased due to over-reporting and misdiagnosis (Victora et al., 2016). French Polynesian researchers subsequently retrospectively identified an increase in the number of fetal abnormalities, including microcephaly, following the outbreak of zika virus in the country (Cauchemez et al., 2016; Jouannic et al., 2016).

The close similarity between ZIKV and other well-studied Flaviviruses such as West Nile Virus (WNV), Promote Encephalitis Virus (JEV), dengue virus (DENV) and tick-borne encephalitis virus (TBEV) has facilitated research and vaccine development (Davis et al., 2001; Monath et al., 2003; Putnak et al., 1996). The experience gained from 20 years of research on these flaviviruses has led to vaccine design and suggests that protection against ZIKV may be carried out via anti-bodies that bind to envelope protein (Nowakowski et al., 2016). Several vaccine candidates are currently under development. These consist of viral vectored vaccines, purified inactivated viruses (PIV's), mRNA vaccines, live attenuated viruses (LAV's) and DNA vaccines. These efforts by various laboratories have caused the unprecedented pace of ZIKV vaccine development.

Numerous vaccine candidates have successful preclinical development. Neutralizing antibodies were induced in all mouse tested vaccines. All vaccines could provide short term protection in mice against ZIKV challenges. To date, DNA, mRNA, PIV and ad-based vaccines have also protected monkeys. There has also been rapid progress of these candidates in Phase I clinical trials(Barrett, 2016). To date, there are 13 open clinical trials testing the ZIKV vaccine concept including DNA vaccines, mRNA vaccines, PIV vaccines, and viral vector-based vaccines.

There is still a lack of effective vaccines and specific medicines to combat the ZIKV infection. Nevertheless, several precautionary measures have been prescribed to counter ZIKV contamination, consisting of drinking plenty of water to avoid dehydration, utilization of acetaminophen or paracetamol to diminish the torment and fever, etc. However, these precautionary measures are insufficient to prevent ZIKV transmission; that is the reason there is an earnest need to look for efficient vaccine development. To plan a viable vaccine effective against different ZIKV strains, it is necessary to select numerous epitopes that are antigenic and then add the suitable adjuvant to improve immune reaction in the host. A subclass of the vaccine family, a subunit vaccine can fulfill the above-mentioned attributes of the immunization (Kumar Pandey et al., 2018).

With recent advances in technology and bioinformatics, MEBP has become a new path to predicting possible epitopes and obtaining cell-mediated (CTL &HTL) and humoral immunity (B cell) (Khatoon et al., 2017; Kumar Pandey et al., 2018; Li et al., 2017; Pandey et al., 2018; Stasyk and Huber, 2016). This investigation additionally implies the utilization of immunoinformatics tools and ways to produce the subunit vaccine with a capacity to evoke explicit T- and B-cell immune reactions against ZIKV infection. ZIKV proteins have been selected to predict epitopes of B cells, T cells and IFN- γ. High antigenic and conserved epitopes were screened out and then merged with linkers and adjuvant to design subunit vaccine. Physicochemical properties, allergenicity, structural detail, and antigenicity of the vaccine were analyzed by online tools. Further, docking was performed among vaccine and TLR-3. *In-silico* cloning was ultimately carried out to probe the advanced polyprotein formation.

2. Methodology

2.1. Retrieval of proteins sequences of ZIKV

In the first step, ZIKV structural and non-structural proteins were retrieved from GENBANK(Benson et al., 2008) in FASTA format.

2.2. Analysis of the ZIKV proteins physicochemical and secondary structural properties

To evaluate the physicochemical properties of ZIKV proteins, the expassy protparam tool was used. Vaxijen 2.0 database was also used to test the protein's antigenicity (Doytchinova and Flower, 2007). The threshold value was maintained at 4.0 and the secondary structure of the target protein was predicted via the SOPMA tool (Deléage, 2017).

2.3. Homology modeling and validation

For modeling the three- dimensional structures of the target proteins, homology modeling servers (Swiss Model (Waterhouse et al., 2018), Phyre 2 (Kelley et al., 2015) and Raptor x (Peng and Xu, 2011) were used. Then the retrieved models were improved by the Galaxy refine server. To know the quality and accuracy of the models, they were subjected to Ramachandran plot analysis by Rampage Server (Lovell et al., 2003).

2.4. Epitope prediction

The inducing epitopes (B-cell, T cell, and IFN-γ) were predicted using the amino acid sequences of proteins.

2.4.1. Prediction of T cell epitope

2.4.1.1. CTL epitopes. NetCTL.1.2 database was used to determine the 9-mer T-cell epitopes recognized by the commonly occurring HLA class 1 supertypes in human population i-e A1, A2, A3, A24, A26, B7, B8, B27, B39, B44, B58, and B62 (Larsen et al., 2007). The thresholds for parameters such as proteasomal C-terminal cleavage, epitope recognition, and transporter associated with antigen processing (TAP) transport efficiency are set in the NetCTL.1.2 database respectively at 0.15, 0.75, and 0.05.

2.4.1.2. HTL epitopes. Net MHC II pan 3.2 (Jensen et al., 2018) and IEDB consensus method (Wang et al., 2010) were utilized to determine the 15-mer T cell epitopes for mouse alleles namely H2IAb, H2IAd, H-2-IAs, H-2-IEd, and H-2-IEk. Peptides were categorized as strong, intermediate and non-binding on the basis of percentile rank. The threshold was set at 2%, 10% and correspondingly higher than 10% for strong, intermediate and non-binding.

2.5. Prediction of B-cell epitope

B cell epitopes help to activate the immune system to detect virus infection. An online tool of ABCPred was used to predict 14-mer B-cell epitopes for all ZIKV proteins. The minimum value was set at 0.51 respectively (Saha and Raghava, 2006).

2.6. Peptides immunogenicity prediction

The Vaxijen v2.0 tool was utilized to analyze the T cell and B cell epitopes 'antigenicity. The antigenic epitopes were selected at the threshold value of 4.0, while non-antigenic epitopes were eliminated.

2.7. Peptides conservation analysis

The Immune Epitope Database (IEDB) was used to monitor the degree of conservation in the protein sequences of the predicted B cell and T cell epitopes (Bui et al., 2007). For further analysis, epitopes showing 100% conservation were selected.

2.8. Interferon-gamma for the analysis of epitopes

IFN-γ is known to elicit responses and can directly detain viral replication. Besides, they can validly evoke the versatile immune reaction by activating cytotoxic T cells and T helper cells. IFN epitope server predict IFN-γ epitopes of selected proteins of ZIKV using SVM hybrid algorithms along with Motif (Dhanda et al., 2013).

2.9. MEBP vaccine sequence construction

The HTL and CTL epitopes selected from 6 ZIKV proteins were merged to make the final vaccine construct. The selected epitopes should harbors the features such as be conserved, overlapping and immunogenic. β-defensin in mammals has a role as a mucosal adjuvant against HIV infection, so it was added to the N-terminal of the vaccine construct because of its adjuvant properties against viral infection (Mohan et al., 2014; Mohan et al., 2013). The adjuvant and first CTL epitope were combined with the support of the EAAAK linker, while AAY and GPGPG linkers were utilized to join other CTL and HTL epitopes respectively.

2.10. Different physicochemical properties prediction of vaccine construct

ProtParam tool was utilized to determine the physicochemical properties of the multi-epitope vaccine (Walker, 2005). It predicts different physicochemical attributes such as (theoretical pI, Grand Average Hydropathy, Stability Profiling, Instability Index, Half-Life and Aliphatic Index) that are dependent on the pK approximations of amino acids involved (Bjellqvist et al., 1993).

2.11. Prediction of allergenicity and antigenicity

Allergic and non-allergic nature of the vaccine was evaluated using the AllerTOP V2.0 server (Dimitrov et al., 2013). This utilizes the data protein sequence by applying k-nearest neighbor calculation (kNN; k = 3) based on recommendations with 2210 non-allergens of similar species and 2210 allergens of different species. Vaxijen server was used to predict the vaccine's antigenicity (Doytchinova and Flower, 2007). This identification depends on different physicochemical attributes of protein and is alignment-free in vaxijen.

2.12. Secondary structure prediction of vaccine constructs

SOPMA has been used to determine the vaccine's secondary structure (Deléage, 2017). The level of beta-turn, extended strand, alpha helices, and random coils were assessed by this tool. The results retrieved is in the form of two graphs. One depicting the prediction and the second showing score curves for all predicted positions.

2.13. Tertiary structure prediction and refinement of vaccine construct

SWISS-Model is a server for showing protein automated homology (Waterhouse et al., 2018). It was used to depict the tertiary structure arrangement of the predicted vaccine. It allows the client to construct the homology model at certain points of unpredictability. The protein homology model was developed based on the quality of the QMEAN model. It gives results as QMean value and GMQE value. GMQE (Global Model Quality Estimation) reflects the certainty of a model by taking into account the coverage, template, and arrangement of the target. It also offers a calculation of quality by combining target-template alignment properties with the template search method. The higher the GMQE value, the better the model's quality. It is usually calculated in 0 and 1 range and GalaxyRefine server (Shin et al., 2014) have been used to optimize the Swiss model's tertiary vaccine structure. It generates several models with deviations in the structure given. Ramachandran plot was made by online server RAMPAGE to authenticate the tertiary structure of the developed vaccine (Lovell et al., 2003). The result of RAMPAGE predicts the nature of the retrieved structure which comprises a number of residues present in outlier and allowed regions. PROSA analysis is further performed for protein structure validation (Wiederstein and Sippl, 2007). This included the evaluation for the defined structure of a general quality score. If the PROSA score for local proteins reaches the specific limit, it is a false score for the structure.

2.14. Molecular docking of TLR 3 with MEBP vaccine candidate

The interaction between the immune receptor and the antigenic molecule is required to produce an effective immune reaction. Molecular docking was performed to assess the binding interaction among ligand (subunit vaccine) and immune receptors. To confirm the immune reactions, HDOCK was used to dock the final MEBP vaccine and TLR-3. It is a web server modeling based on templates that is based on the hybrid docking procedure and takes structure and sequence inputs for protein. It supports protein-protein docking and protein-DNA/RNA docking(Yan et al., 2017) (Fig. 1).

2.15. In-silico cloning

Codon optimization and reverse translation are evaluated using the codon adaptation tool to predict appropriate expression in vector translation and efficiency of cloning(Grote et al., 2005). *Escherichia coli* (K-12 strain) has been identified as a host organism for the expression of vaccine construct. Results were generated in graphical representation and the form of codon adaptive index (CAI) values. The detail of tools used in this study are give below in Table 1

3. Results

3.1. Protein targets

The amino acid sequences of seven non-structural proteins (NS1 [Genbank: YP_009227199.1], NS2A [Genbank: YP_009227200.1], NS2B [Genbank: YP_009227201.1], NS3 [Genbank: YP_009227202.1], NS4A [Genbank: YP_009227203.1], NS4B [Genbank: YP_009227204.1], and NS5 [Genbank: AJD79014.1]) and three structural Proteins (Capsid(C) [Genbank: YP_009430296.1], Envelope (E) [Genbank: ASN64427.1], Membrane (prM/M) [Genbank: YP_009227197.1]) were retrieved from Genbank in FASTA format. Further, their antigenicity was checked by Vaxijen 2.0 tool. The threshold value was kept at 0.4. Vaxijen 2.0 tool found the NS2A as the most antigenic protein followed by E, NS4A, prM/M, NS2B, NS4B, NS5, NS3 and NS1 having antigenic values of 0.6461, 0.6237, 0.5998, 0.5776, 0.5748, 0.5444, 0.5091, 0.4958 and 0.4455 respectively. Capsid protein was found to be non-antigenic so it was excluded. Besides, to identify non-homologous proteins, Blast p analysis was performed against *Homo sapiens* with default parameters. Proteins having an identity- < 37% were considered as non-homologous proteins. NS3, NS5 and prM/M showed 50%, 43.2% and 37.14% similarity with the human proteome. So these three proteins were excluded from the analysis. Five Non-structural proteins (NS1, NS2A-2B, and NS4A-4B) and one structural protein (Envelope E) were selected as targets for further analysis. Other physicochemical characters like theoretical pI, molecular weight, half-life, stability profiling, aliphatic index, etc. (Table 2) and secondary structure properties were also predicted (Table 3).

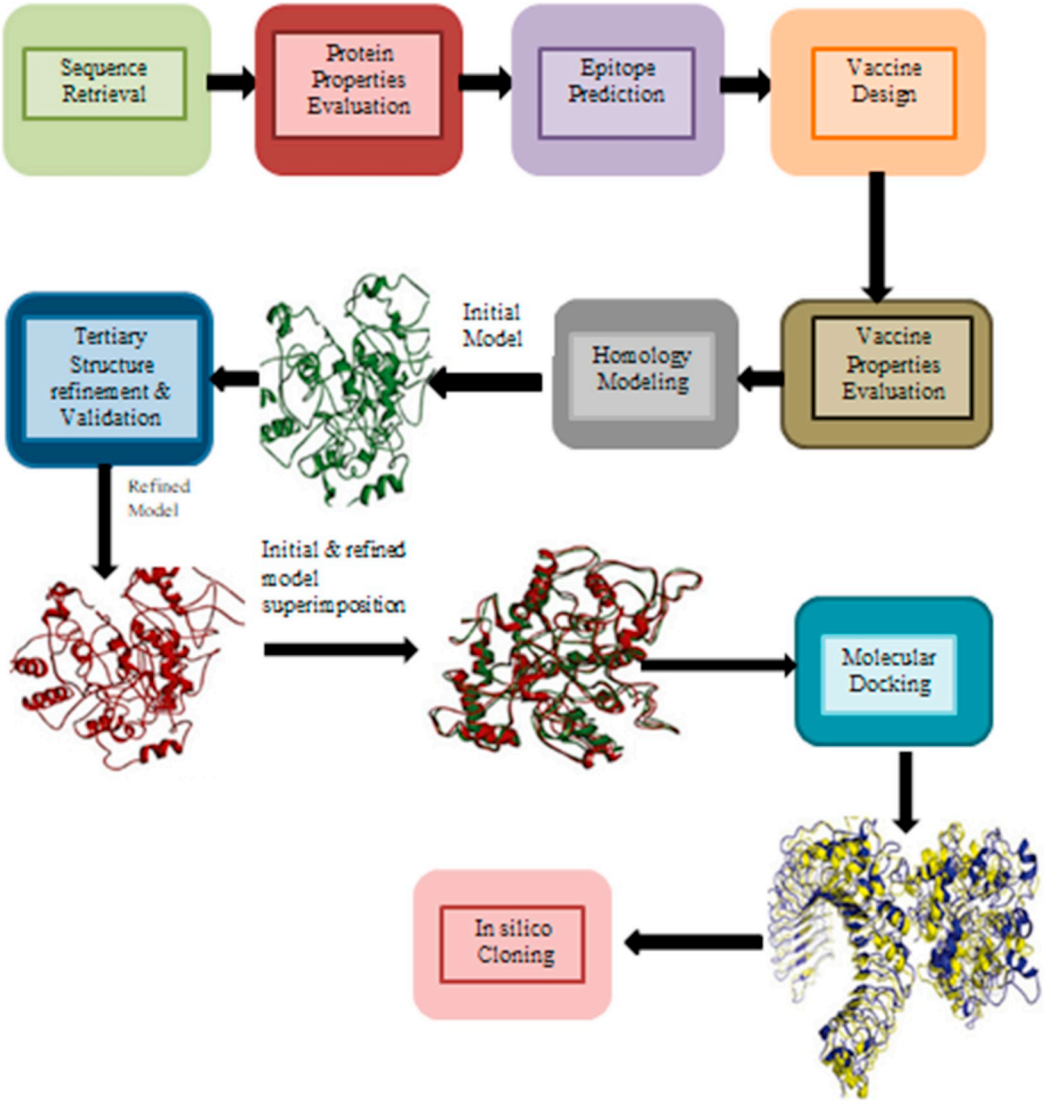

Fig. 1. Schematic representation of methodology used in study.

3.2. Homology modeling and validation

Ramachandran plot analysis evaluated the 3D models retrieved through Phyre 2, Raptor X and Swiss model homology modeling methods. The specificity and reliability of the models were evaluated using various homology modeling tools. Compared to those from other homology modeling tools such as the Swiss model and Phyre-2, the Raptor-X models were of better quality and showed good Ramachandran plots. Specific statistics were also noted on the alignment of target protein models. In addition, the models were also subjected to Galaxy refine tool for refinement (Table 4).

3.3. Prediction of T cell epitope

The NetCTL 1.2 was used to predict CTL epitopes and to predict HTL epitopes using the Net MHC II pan 3.2 and IEDB consensus system servers. Epitopes that are 100% conserved in protein sequence and antigenic were selected. Total 39 CTL epitopes (E-11, NS1–6, NS2A-5, NS2B-5, NS4A-6, and NS4B-6) (Table 5) and 41 HTL epitopes (E-8, NS1–5, NS2A-18, NS2B-2, NS4A-1, and NS4B-7) (Table 6) were chosen for further study.

3.4. Prediction of B cell epitope

For all ZIKV proteins, ABCPred has been used to predict linear B-cell epitopes. Just like T-cell epitopes, the B cell epitopes screened out were 100% conserved in nature between protein sequences and antigenic. All target proteins were predicted to have a total of 64 linear epitopes (E-24, NS1–15, NS2A-10, NS2B-1, NS4A-3, and NS4B-11) (Table 7). Furthermore, the Ellipro server was utilized to determine the conformational epitopes. All proteins were predicted to have a total of 33 conformational epitopes (E-3, NS1–6, NS2A-7, NS2B-7, NS4A-5, and NS4B-5) (Table 8).

3.5. MEBP vaccine sequence construction

The conditions for inclusion of the epitopes in the subunit vaccine construct were: (a) T cells overlapping B cell epitopes and IFN-γ epitopes (b) immunogenicity (c) 100% protein sequence conservation. 14 CTL epitopes and 11 HTL epitopes were shortlisted based on these criteria. The final subunit vaccine was developed by linking the epitopes (HTL & CTL) respectively via GPGPG and AAY linkers. There are two roles of GPGPG linkers in the structure of MEBP. First, it avoids the

Table 1
Function and description of the tools used in the study.

Tools	Function	Description	URL
GenBank	Sequence retrieval	GenBank is the NIH genetic sequence database, an annotated collection of all publically available DNA and protein sequences.	https://www.ncbi.nlm.nih.gov/genbank/
ProtParam	Physiochemical properties evaluation	It surveys different physicochemical attributes (theoretical pI, Grand Average Hydropathy, Stability Profiling, Instability Index, Half-Life and Aliphatic Index) that are dependent on the pK approximations of amino acids involved.	https://web.expasy.org/protparam/
Vaxijen 2.0	Antigenicity testing	Vaxijen is the first server for predicting the independent alignment of protective antigens. It was developed to allow antigen classification based solely on the physiochemical properties of the protein, without resorting to sequence alignment.	http://www.ddg-pharmfac.net/vaxijen/VaxiJen/VaxiJen.html
AllerTOP 2.0 server	Allergenicity testing	AllerTOP is an alignment-free method for in silico allergen prediction based on the main physiochemical properties of protein.	https://www.ddg-pharmfac.net/AllerTOP/
SOPMA	Secondary structure prediction	SOPMA method predicts 69.5% amino acids for a three-state description of the secondary structure (alpha helix, beta-sheet, and coil) of the entire database including 126 chains of non-homologous proteins.	https://npsa-prabi.ibcp.fr/cgi-bin/npsa:automat.pl?page=/NPSA/npsa:sopma.html
Phyre 2	Tertiary structure prediction	Phyre 2 is a web-based toolkit for predicting and analyzing protein structure, function, and mutation.	http://www.sbg.bio.ic.ac.uk/~phyre2/html/page.cgi?id=index
Swiss model	Tertiary structure prediction	Swiss Model is a fully automated protein structure homology modeling server. The purpose of this server is to give all life science researchers worldwide access to protein modeling.	https://swissmodel.expasy.org/
Raptor X	Tertiary structure prediction	RaptorX is developed by Xu group, excelling at secondary, tertiary and contact prediction for protein sequences without close homologs in the Protein Data Bank (PDB).	http://raptorx.uchicago.edu/
NetCTL.1.2 server	CTL epitope prediction	NetCTL is a web-based tool designed to predict human CTL epitopes for specific proteins. This is done by integrating proteasome cleavage prediction, TAP transport efficiency and MHC class I affinity.	http://www.cbs.dtu.dk/services/NetCTL/
Net MHC II pan 3.2 server	HTL epitope prediction	Net MHC II pan 3.2 server provides peptide binding to MHC class II molecules. The prediction is available for three human MHC class II isotypes, HLA-DR, HLA-DP, HLA-DQ, and mouse (H-2) molecules.	http://www.cbs.dtu.dk/services/NetMHCIIpan/
IEDB consensus method	HTL epitope prediction	This tool employs different methods to predict MHC Class II epitopes, including a consensus approach which combines NN-align, SMM-align and Combinatorial library methods.	http://tools.iedb.org/mhcii/
ABCPred	Linear B Cell epitope prediction	ABCPred server is used to predict B cell epitopes within an antigen sequence using artificial neural networks.	http://crdd.osdd.net/raghava/abcpred/
ElliPro Server	Conformational B cell epitope prediction	ElliPro is a web-based tool for the prediction of antibody epitopes in protein antigens of a given sequence or structure. It implements a previously developed method that represents the protein structure as an ellipsoid and calculates protrusion indexes for protein residues outside of the ellipsoid.	http://tools.iedb.org/ellipro/
The immune epitope database (IEDB) conservancy analysis tool	Conservancy analysis	This tool calculates the degree of conservancy of an epitope within a given protein sequence set at different degrees of sequence identity. The degree of conservation is defined as the	http://tools.iedb.org/conservancy/

(*continued on next page*)

Table 1 (*continued*)

Tools	Function	Description	URL
		fraction of protein sequences containing the epitope at a given identity level.	
IFN epitope server	IFN-γ epitope prediction	This module generates overlapping peptides of the query protein/antigen sequence and predicts IFN-gamma inducing ability of these antigenic regions. It allows users to identify regions in a protein/antigen have the potency to induce IFN-gamma.	http://crdd.osdd.net/raghava/ifnepitope/
Galaxy refine server	Refinement of tertiary structure	A web server to improve the structure of protein models. It is particularly effective in improving the quality of local structures as demonstrated by the CASP refinement category.	http://galaxy.seoklab.org/
ModRefiner	Refinement of tertiary structure	ModRefiner is an algorithm for atomic-level, high-resolution protein structure refinement, which can start from either C-alpha trace, main-chain model or full-atomic model	https://zhanglab.ccmb.med.umich.edu/ModRefiner/
RAMPAGE SERVER	Validation of tertiary structure	Rampage server is used for the validation of 3d structure modeled by plotting Ramachandran plot.	http://mordred.bioc.cam.ac.uk/~rapper/rampage.php
PROSA	Validation of tertiary structure	The PROSA (Protein Structure Analysis) program is an established tool with a large user base, often used to improve and validate experimental protein structures and to predict and model structures.	https://prosa.services.came.sbg.ac.at/prosa.php
HDOCK	Molecular docking	It is a web server modeling based on templates that trail the hybrid docking procedure and takes structure and sequence inputs for protein. It supports protein-protein docking and protein-DNA/RNA docking.	http://hdock.phys.hust.edu.cn/
JAVA CODON ADAPTATION TOOL	In silico cloning	Codon optimization and reverse translation are evaluated using the codon adaptation tool to approve appropriate expression in vector translation and efficiency of cloning.	http://www.jcat.de/

generation of junctional epitopes, which is a major concern in the design of the epitope vaccines; and second, it facilitates immunization and presentation of HTL epitopes(Livingston et al., 2002; Nezafat et al., 2016). The AAY motif was used as a linker to join the CTL epitopes (Bergmann et al., 1996). The final vaccine was 385 amino acids long after merging. Moreover, the EAAAK linker was used to attach 45 amino acid long β-defensin as an adjuvant to the N-end of the vaccine. An adjuvant was added to enhance the immunogenicity of the vaccine. EAAAK linker was used to bind the adjuvant and CTL epitope to the N-terminal of the vaccine structure, reducing interaction with other protein regions with efficient separation(Arai et al., 2001; Pandey et al., 2017). The final construct was 435 amino acids long after the addition

Table 2
Physiochemical properties of the ZIKV proteins analyzed through protparam tool.

Proteins	Molecular weight	Theoretical pI	Instability index	Half -life	Stability profiling	Aliphatic index	Grand average of hydropathy
E protein	54334.11	6.52	22.44	20 h (mammalian reticulocytes, in vitro). 30 min (yeast, in vivo). > 10 h (*Escherichia coli*, in vivo).	Stable	81.45	−0.088
NS1	40078.36	6.17	39.64	1.1 h (mammalian reticulocytes, in vitro). 3 min (yeast, in vivo). > 10 h (Escherichia coli, in vivo).	Stable	68.89	−0.553
NS2A	23965.12	10.34	28.06	30 h (mammalian reticulocytes, in vitro). > 20 h (yeast, in vivo). > 10 h (Escherichia coli, in vivo).	Stable	132.52	0.888
Ns2B	13777.03	4.44	29.08	1.9 h (mammalian reticulocytes, in vitro). > 20 h (yeast, in vivo). > 10 h (Escherichia coli, in vivo).	Stable	103.54	0.403
NS4A	13696.46	5.82	37.25	30 h (mammalian reticulocytes, in vitro). > 20 h (yeast, in vivo). > 10 h (Escherichia coli, in vivo).	Stable	122.91	0.684
NS4B	26943.52	9.10	38.61	1.4 h (mammalian reticulocytes, in vitro). 3 min (yeast, in vivo). > 10 h (Escherichia coli, in vivo).	Stable	101.95	0.339

Table 3
Secondary structure of the ZIKV proteins predicted via SOPMA.

Proteins	Sequence length	α-helix	β-Turn	Random coils
Envelope	504	19.84%	7.14%	42.06%
NS1	352	25.28%	7.6%	47.73%
NS2A	226	58.41%	8.85%	17.26%
NS2B	130	40.77%	5.38%	33.08%
NS4A	127	54.33%	8.66%	18.11%
NS4B	251	54.58%	8.37%	24.70%

Table 4
Structural details of the ZIKV proteins model.

Proteins	Tool utilized for modeling	Template	Ramachandran plot		
			Favored region	Allowed region	Disallowed region
E	Raptor x	5gzrA	95.2%	4.0%	0.8%
NS1	Raptor x	5gs6A	96.9%	2.3%	0.9%
NS2A	Raptor x	4he8G	92.4%	5.8%	1.8%
NS2B	Raptor x	5lc0A	100%	0.0%	0.0%
NS4A	Raptor x	5cwoA	96.8%	1.6%	1.6%
NS4B	Raptor x	4av3A	92.8%	4.4%	2.8%

Table 5
CTL Epitopes. The epitopes listed in the table showed 100% conservancy (as predicted by IEDB conservancy analysis tool) among the protein sequences included in the present study.

Protein	Peptide (Position)	Antigenicity
E Protein	GLDFSDLYY (195–203)	1.7
	FSDLYYLTM (198–206)	0.7
	SIQPENLEY (129–137)	2.1
	STENSKMML (368–376)	0.4
	TMNNKHWLV (205–213)	1.0
	GTVTVEVQY (324–332)	1.4
	GLFGKGSLV (106–114)	0.8
	RLKGVSYSL (299–307)	1.1
	KLRLKGVSY (297–305)	1.8
	HWHRSGSTI (399–407)	0.4
	AKRQTVVVL (250–258)	0.8
	EAAHSDLGY (192–200)	1.3
NS1	HSEELEIRF (269–277)	1.3
	RAAKTNNSF (125–133)	0.6
	WRLKRAHLI (210–18)	1.1
	GREAAHSDL (190–198)	0.9
	LEHRAWNSF (145–153)	0.7
NS2A	VMALGLTAV (198–206)	1.3
	LLVAWRAGL (166–174)	0.5
	IALPILAAL (150–158)	0.4
	AFKVRPALL (82–90)	1.5
	VPRTDNIAL (144–152)	
NS2B	YVYVKTGKR (122 – 130)	1.0
	GPPMREIIL (91–99)	0.4
	LDESGDFSL (78–86)	0.7
	DESGDFSLV (79–87)	1.1
	GMNPIAIPF (108–116)	1.1
NS4A	LMRNKGIGK (72–80)	0.5
	VFLLLVVLI (112 – 120)	0.5
	CVLIVVFLL (107–115)	0.4
	EPARIACVL (101–109)	1.0
	MRNKGIGKM (73–81)	1.0
	KMGFGMVTL (80–88)	1.6
NS4B	ILLVAHYMY (114–122)	0.6
	YLIPGLQAA (122–130)	0.9
	LLVAHYMYL (115–123)	0.5
	AIILLVAHY (112–120)	0.5
	AVAISSAVL (177–185)	0.4
	SAVLLRTAW (182–190)	0.7

of linkers and adjuvant. (Fig. 2).

3.6. Linear and conformational B epitopes and other physicochemical properties of the vaccine

ABCPred 2.0 and Ellipro servers were used to predict linear/continuous and conformational/discontinuous B cell epitopes in the vaccine model without altering any prediction parameters. The servers predicted 30 linear/continuous (Table 10) and 3 conformational/discontinuous B cell epitopes (Table 9). The ProtParam server different physicochemical characteristics of the final vaccine. The PI of the vaccine was 9.61, depicting it as basic while its molecular weight is 46,477.79 g/mol. The estimated aliphatic index is 84.78 depicting it as thermostable. The construct's average half-life was measured as 30 h in vitro (in mammalian reticulocytes), whereas in vivo (*Escherichia coli* & yeast) it is estimated as > 20 h and > 10 h respectively. 0.12 was calculated as a grand average of hydropathcity (GRAVY); the score in positive designate its hydrophobic nature.

3.7. Prediction of allergenicity and antigenicity

Vaccine allergenicity was anticipated by utilizing AllerTOP 2.0 server. AllerTOP demonstrates the vaccine's non-allergenic behavior. The antigenicity of the subunit vaccine was predicted with Vaxijen v2.0. The antigenicity of the vaccine was 0.6548 according to vaxijen at the threshold value of 0.4% which indicates the antigenic nature of the vaccine.

3.8. Prediction of secondary structure

SOPMA has been used to analyze the vaccine's secondary structure. SOPMA predictions depend on the amino acids of the vaccine sequence. Among 435 amino acids, 167 amino acids participate in the formation of α-helix which accounts for 38.39%, 31 in β-strands which are 7.13% and coils are formed by 141 amino acids which are 32.41% of the whole vaccine construct. (Fig. 3) SOPMA consists of various parameters, for example, number of conformational states, window width and so on that is used for the prediction.

3.9. 3D structure prediction, refinement and validation

The Swiss model was used to estimate the tertiary structure of the vaccine (Fig. 4A). The GMQE was 0.04 and Q mean was −2.88 depicting the high quality of the vaccine. Using the mod refiner and then Galaxy Refine server, the tertiary structure of the vaccine has been improved. GalaxyRefine produces 5 models after refinement. After observing scores of 5 models, model 4 was observed to be the finest model and it was chosen for further analysis (Fig. 4B). The improved model exhibits a 95% favored region in RAMPAGE and qRMSD as 0.447, poor rotamers as 2.6, MolProbity as 1.913, clash score as 10.3 and RAMPAGE server analyzes and validates the tertiary structure by producing Ramachandran plot. According to the Ramachandran plot generated for vaccine construct, there are 97.7% of residues in the most favored region, 2.3% of amino acids reside in the allowed region, and 0.0% are displayed in outlier regions. (Fig. 4D) Additionally, ProSA-web gives a − 4.71 Z score that lies inside the range of acceptable scores (Fig. 4C).

3.10. Molecular docking of the immunological receptor (TLR-3) and vaccine candidate

The activation of an immune response requires an appropriate association among immune receptor molecules along with the antigenic

Table 6
HTL Epitopes. The boxes colored with blue, light grey and black shows the strong, intermediate and non-binding affinities towards the respective mouse H-2 alleles.

Protein	Peptide Position	Peptide Sequence	Mouse (H-2) Alleles					Antigenicity
			H-2-IAb	H-2-IAd	H-2-IAs	H-2-IEd	H-2-IEk	
E protein	410-424	AFEATVRGAKRMAVL						0.6
	411-425	FEATVRGAKRMAVLG						0.9
	198-212	FSDLYYLTMNNKHWL						0.9
	201-215	LYYLTMNNKHWLVHK						0.6
	202-216	YYLTMNNKHWLVHKE						0.7
	199-213	SDLYYLTMNNKHWLV						0.8
	200-214	DLYYLTMNNKHWLVH						0.8
	203-217	YLTMNNKHWLVHKEW						0.9
NS1	121-135	SYFVRAAKTNNSFVV						0.6
	122-136	YFVRAAKTNNSFVVD						0.5
	207-221	NDTWRLKRAHLIEMK						0.7
	208-222	DTWRLKRAHLIEMKT						0.4
	209-223	TWRLKRAHLIEMKTC						0.4
NS2A	78-92	ALVAAFKVRPALLVS						1.1
	79-93	LVAAFKVRPALLVSF						1.2
	130-144	NGFALAWLAIRAMAV						0.7
	131-145	GFALAWLAIRAMAVP						1.0
	132-146	FALAWLAIRAMAVPR						0.9
	133-147	ALAWLAIRAMAVPRT						0.9
	134-148	LAWLAIRAMAVPRTD						0.9
	135-149	AWLAIRAMAVPRTDN						0.8
	149-163	NIALPILAALTPLAR						0..6
	150-164	IALPILAALTPLARG						0.8
	151-165	ALPILAALTPLARGT						1.1
	152-166	LPILAALTPLARGTL						0.9
	90-104	LVSFIFRANWTPRES						1.3
	91-105	VSFIFRANWTPRESM						1.4
	92-106	SFIFRANWTPRESML						1.2
	93-107	FIFRANWTPRESMLL						1.2
	94-108	IFRANWTPRESMLLA						0.9
	136-150	WLAIRAMAVPRTDNI						0.8
NS2B	110-124	NPIAIPFAAGAWYVY						0.6
	111-125	PIAIPFAAGAWYVYV						0.5
NS4A	92-106	AWLMWLSEIEPARIA						0.7
NS4B	118-132	AHYMYLIPGLQAAAA						0.7
	119-133	HYMYLIPGLQAAAAR						0.6
	120-134	YMYLIPGLQAAAARA						0.5
	188-202	TAWGWGEAGALITAA						0.8
	189-203	AWGWGEAGALITAAT						0.6
	190-204	WGWGEAGALITAATS						0.7
	175-189	LIAVAISSAVLLRTA						0.5

Table 7
Linear B cell epitopes predicted through ABCPred 2.0 server.

Proteins	B cell (Position)	Antigenicity
E protein	TVRGAKRMAVLGDT (414)	0.6
	PAQMAVDMQTLTPV (342)	0.6
	LRLKGVSYSLCTAA (298)	0.7
	DSRCPTQGEAYLDK (71)	0.4
	NSKMMLELDPPFGD (371)	0.7
	SDLYYLTMNNKHWL (199)	0.8
	WDFGSVGGALNSLG (429)	1.1
	GAKGRLSSGHLKCR (279)	1.4
	VDRGWGNGCGLFGK (97)	0.5
	EALVEFKDAHAKRQ (240)	0.8
	DIPLPWHAGADTGT (220)	0.4
	RAKVEITPNSPRAE (164)	0.7
	HAGADTGTPHWNNK (226)	0.8
	PNSPRAEATLGGFG (171)	0.6
	PHWNNKEALVEFKD (234)	1.5
	KMTGKSIQPENLEY (124)	1.4
	KRQTVVVLGSQEGA (251)	0.8
	CEPRTGLDFSDLYY (190)	0.9
	YIVIGVGEKKITHH (386)	1.3
	PPFGDSYIVIGVGE (380)	0.8
	MNNKHWLVHKEWFH (206)	0.4
	TLGGFGSLGLDCEP (179)	1.6
	VVLGSQEGAVHTAL (256)	0.5
	KAFEATVRGAKRMA (409)	0.4
NS1	HSDLGYWIESEKND (195)	0.5
	VWLKVREDYSLECD (167)	0.7
	HHNTREGYRTQVKG (253)	0.5
	LEENGVQLTVVVGS (79)	0.4
	QVKGPWHSEELEIR (263)	0.9
	AGPLSHHNTREGYR (248)	0.8
	TAVKGREAAHSDLG (186)	1.2
	CDPAVIGTAVKGRE (179)	1.1
	GFGVFHTSVWLKVR (159)	0.5
	VQLTVVVGSVKNPM (84)	0.7
	SLRSTTASGRVIEE (297)	0.5
	HSEELEIRFEECPG (269)	0.6
	YFVRAAKTNNSFVV (122)	0.6
	GTKVYVEETCGTRG(282)	0.4
	TLKECPLEHRAWNS (139)	0.6
NS2A	DNIALPILAALTPL (148)	0.5
	LVAAFKVRPALLVS (79)	1.2
	FIFRANWTPRESML (93)	1.2
	LAALTPLARGTLLV (155)	0.9
	LAWLAIRAMAVPRT (134)	1.0
	CGGIMLLSLKGKGS (177)	0.8
	LKGKGSVKKNLPFV (185)	0.9
	CGGIMLLSLKGKGS (177)	0.8
	RPALLVSFIFRANW (86)	0.9
	ARGTLLVAWRAGLA (162)	0.6
NS2B	ALDESGDFSLVEED (77)	0.6
NS4A	KMGFGMVTLGASAW (80)	1.2
	LGASAWLMWLSEIE (88)	0.4
	IEPARIACVLIVVF (100)	1.1
NS4B	SQLTPLTLIVAIIL (102)	0.7
	KMGQVLLIAVAISS (169)	0.6
	VAISSAVLLRTAWG (178)	0.5
	DPQVEKKMGQVLLI (163)	0.5
	PFMHGDLGVPLLMM (85)	0.6
	AIILLVAHYMYLIP (112)	0.6
	LTLIVAIILLVAHY (107)	0.4
	VAHYMYLIPGLQAA (117)	0.7
	GVLFGMGKGMPFMH(75)	0.4
	YLIPGLQAAAARAA(122)	0.4
	TAWGWGEAGALITA (188)	0.8

molecule. Thus for the execution of docking analysis of the construct with TLR3, HDOCK server was used. In the docked complex, pink color depicts the vaccine molecule, while the rainbow color depicts the TLR3 (Fig. 5).

3.11. In silico cloning

An online server, Codon adaptation tool, was used to generate a cDNA sequence followed by codon optimization analysis which evaluates codon adaptive index (CAI) and GC data. The GC content of the construct was yielded as 55.40% which resides in the ideal range (30–70%), and CAI as 1.0 that additionally resides in the value (0.8–1.0) that depicts the efficient expression of the protein potentiating its reliability.

4. Discussion

Vaccination has many effective ways to improve public health in a cost-effective manner and leading means to prevent spread of infectious diseases in the world. Current researchers are seeking methods to develop subunit vaccines for whole-organism vaccines since subunit vaccines contain different immunogenic components of the disease-causing pathogens, rather than the entire pathogenic agent (Khatoon et al., 2017). The use of computational tools for antibody epitope prediction represents one of the appreciable phases of designing a vaccine (Dubey et al., 2018).

Immunoinformatics as subdivision of bioinformatics that encompasses with a variety of tools and databases for in silico analysis and prediction of immunological dataset. The availability of genomic, immunological data and software algorithms has facilitated in more efficient vaccine development process that allows scientists to identify the effective epitopes that can be used to develop active subunit vaccines (De Gregorio and Rappuoli, 2012; Patronov and Doytchinova, 2013; Yang and Yu, 2009). Immunoinformatics methodologies serve as a corner-stone in the pace for subunit vaccines based on the prediction of B-cell and T-cell epitopes (Gillespie et al., 2000).

However, there are some limitations compared to traditional experimental approaches. With the help of immunoinformatics, it is possible to analyze the full range of potential antigens. In addition, the viability of pathogen culture and the problem of in vitro antigen expression can be avoided, and some of the in silico candidates reported by the immunological research is known to have promising preclinical results (Davies and Flower, 2007). The In silico procedures helps to reduce the number of in vitro experiments (Mirza et al., 2016). It also saves time, overcomes cost obstacles and increases the potential for successful vaccine design (Khan et al., 2018). A Multi-epitope vaccine containing a series of peptides that induce activation of humoral and adaptive immune responses is an ideal strategy for prevention and treatment of viral or tumor infections (Brennick et al., 2017; Chauhan et al., 2019; He et al., 2018; Lu et al., 2017). As compared to traditional vaccines, multi-epitope vaccines are more immunogenic having fewer or no adverse events (Ojha et al., 2019). The design of the epitope vaccine construct against HIV (Kumar Pandey et al., 2018), Chikungunya (Tahir ul Qamar et al., 2018), Ebola Virus (Ahmad et al., 2019) and HCV (Ikram et al., 2018) have yielded promising results while maintaining a defensive approach and therapeutic potency of the developed vaccines candidate.

To date, the lack of therapeutic or approved ZIKV vaccines has exacerbated infection control and prevention. There are significant efforts to improve awareness of ZIKV's vulnerability and pathogenesis (Malet et al., 2008; Perera et al., 2008). Risks associated with autoimmune responses need to be considered in the development of Zika virus infection vaccines and therapies (Homan et al., 2016).

The aim of this study is to establish a MEBP vaccine to improve safety against ZIKV. Two subunit vaccines against ZIKV were reported by using the immunoinformatics approach where they have used three proteins for vaccine development (Kumar Pandey et al., 2018; Mirza et al., 2016). Both studies use three proteins for ZIKV vaccine development, but this study included more number of proteins and epitopes.

Table 8
Conformational B cell epitopes of ZIKV proteins predicted by Ellipro server.

Proteins	Conformational B cell epitopes	3D Structure
	:E62, _:A63, _:S64, _:I65, _:S66, _:D67, _:M68, _:A69, _:S70, _:D71, _:S72, _:R73, _:C74, _:P75, _:T76, _:Q77, _:G78, _:E79, _:A80, _:Y81, _:L82, _:D83, _:K84, _:Q85, _:S86, _:D87, _:T88, _:Q89, _:Y90, _:V91, _:C92, _:K93, _:R94, _:T95, _:L96, _:V97, _:D98, _:R99, _:G100, _:W101, _:G102, _:N103, _:G104, _:C105, _:G106, _:L107, _:F108, _:G109, _:K110, _:G111, _:S112, _:L113,	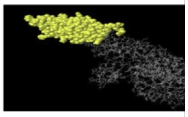
Envelope	_:V114, _:T115, _:G116, _:A117, _:K118, _:F119, _:A120, _:S122, _:K123, _:G228, _:A229, _:D230, _:T231, _:G232, _:T233, _:P234, _:H235, _:W236, _:N237, _:K239, _:E240, _:A241, _:L242, _:V243, _:E244, _:F245, _:K246, _:D247, _:A248, _:H249, _:A250, _:K251, _:R252, _:Q253, _:T254, _:V255, _:V256, _:V257, _:L258	
	G14, _:S16, _:G17, _:G18, _:T19, _:W20, _:Q147, _:H148, _:S149, _:G150, _:N154, _:D155, _:T156, _:G157, _:H158, _:E159, _:T160, _:D161, _:E162, _:N163, _:R175, _:E177, _:L180, _:G181, _:G182, _:F183, _:G184, _:S185, _:K294, _:M295, _:D296, _:K297, _:L298, _:R299, _:L300, _:K301, _:G302, _:V303, _:S304, _:Y305, _:S306, _:L307, _:C308, _:T309, _:A310, _:A311, _:F312, _:T313, _:F314, _:T315, _:K316, _:I317, _:P318, _:E329, _:V330, _:Q331, _:Y332, _:A333, _:G334, _:T335, _:D336, _:G337, _:P338, _:C339, _:K340, _:V341, _:P342, _:Q344, _:A346, _:V347, _:D348, _:M349, _:Q350, _:T351, _:L352, _:T353, _:P354, _:V355, _:G356, _:N362, _:P363, _:V364, _:I365, _:T366, _:E367, _:S368, _:T369, _:E370, _:N371, _:S372, _:K373, _:P380, _:P381, _:F382, _:G383, _:D384, _:S385, _:Y386, _:I387, _:V388, _:I389, _:G390, _:V391, _:G392, _:E393, _:K394, _:K395, _:I396, _:T397, _:H398, _:H399, _:W400, _:H401, _:R402, _:S403, _:G404, _:S405, _:T406, _:I407, _:G408, _:A410, _:F411, _:S433, _:V434, _:G435, _:G436, _:A437, _:L438, _:N439, _:S440, _:L441, _:G442, _:G444, _:I445, _:H446, _:Q447, _:I448, _:F449, _:A451, _:A452, _:F453, _:S455, _:L456, _:F457, _:M460, _:S461, _:F463, _:S464, _:I466, _:L467, _:I468, _:G469, _:T470, _:L471, _:L472, _:M473, _:W474, _:L475, _:G476, _:L477, _:N478, _:T479, _:K480, _:N481, _:G482, _:S483, _:I484, _:S485, _:L486, _:M487, _:C488, _:L489, _:A490, _:L491, _:G492, _:G493, _:V494, _:L495, _:I496	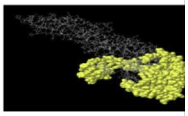
	_:P171, _:N172, _:S173, _:P174	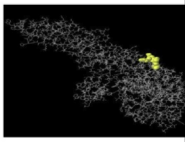
NS1	_:D1, _:V2, _:G3, _:C4, _:S5, _:V6, _:D7, _:F8, _:S9, _:K10, _:E12, _:T13, _:R14, _:C15, _:G16, _:T17, _:G18, _:V19, _:F20	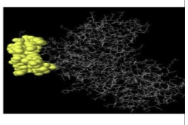
	:D37, _:S38, _:P39, _:R40, _:R41, _:A43, _:A44, _:K47, _:Q48, _:A49, _:W50, _:E51, _:E52, _:G53, _:I54, _:C55, _:G56, _:G73, _:E74, _:N76, _:A77, _:I78, _:L79, _:E80, _:E81, _:N82, _:G83, _:V84, _:Q85, _:L86, _:T87, _:Q102, _:R103, _:L104, _:P105, _:V106, _:P107, _:V108, _:N109, _:E110, _:L111, _:P112, _:H113, _:G114, _:W115, _:K116, _:A117, _:W118, _:G119, _:K120, _:S121, _:Y122, _:F123, _:V124, _:R125, _:A126, _:A127, _:K128, _:T129, _:N130, _:N131, _:S132, _:T139, _:L140, _:C143, _:P144, _:E146, _:H147, _:R148, _:R172, _:E173, _:D174	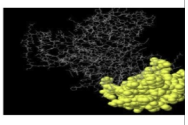
	:P226, _:K227, _:S228, _:H229, _:T230, _:L231, _:W232, _:T233, _:D234, _:G235, _:V236, _:E237, _:E238, _:S239, _:D240, _:L241, _:L251, _:S252, _:H253, _:T256, _:G259, _:Y260, _:R261, _:T262, _:K265, _:E279, _:C280, _:P281, _:G282, _:T283, _:K284, _:V285, _:Y286, _:V287, _:E288, _:E289, _:T290, _:C291, _:G292, _:T293, _:R294, _:G295, _:P296, _:S297, _:L298, _:R299, _:S300, _:T301, _:T302, _:A303, _:S304, _:G305, _:R306, _:V307, _:I308, _:E309, _:E310, _:W311, _:C312, _:C313, _:R314, _:E315, _:C316, _:T317, _:M318, _:P319, _:P320, _:G328, _:G332, _:M333, _:E334, _:I335, _:R336, _:P337, _:R338, _:K339, _:E340, _:P341, _:E342, _:S343, _:N344, _:L345, _:V346, _:R347	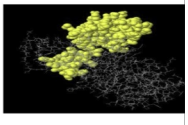
	_:A187, _:V188, _:K189, _:G190, _:R191, _:E192, _:E205, _:K206, _:N207, _:D208, _:T209, _:W210, _:R211, _:K213	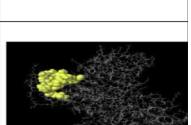

(*continued on next page*)

Table 8 (*continued*)

	_:E156, _:D157, _:H158	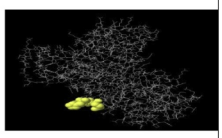
	_:W28, _:R31, _:Y32, _:K33, _:G161, _:F163, _:H164, _:T165	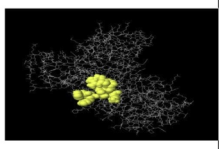
NS2A	_:E22, _:G23, _:K25, _:K26, _:R27, _:M28, _:T29, _:T30, _:K31, _:I32, _:I33, _:M34, _:T36, _:S37, _:E67, _:V214, _:V215, _:G216, _:L217, _:L218, _:L219, _:L220, _:T221, _:R222, _:S223, _:G224, _:K225, _:R226	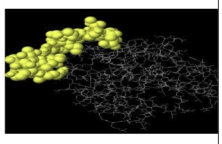
	_:P87, _:L90, _:V91, _:F93, _:I94, _:F95, _:R96, _:W99, _:T100, _:P101, _:R102, _:E103, _:S104, _:M105, _:L106, _:L107, _:M142, _:A143, _:V144, _:P145	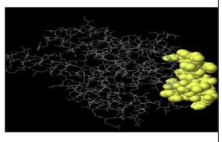
	_:H5, _:M6, _:D7, _:H8, _:L11	
		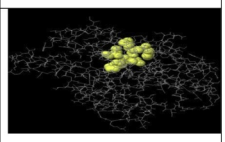
	_:N69, _:T70, _:G71, _:G72, _:D73, _:A75, _:H76, _:V80, _:F83, _:K84, _:R86	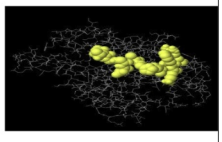
	_:G1, _:S2, _:T3, _:D4, _:G48, _:F49, _:S50, _:S52, _:D53, _:K56	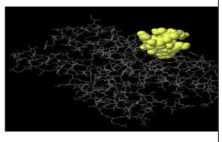
	_:D148, _:N149, _:I150, _:A151, _:L152, _:P153, _:I154, _:A157, _:L158, _:P160, _:L161, _:A162, _:R163, _:G164, _:T165, _:G179, _:I180, _:M181, _:L182, _:L183, _:S184, _:L185, _:K186, _:G187, _:K188, _:G189, _:S190, _:V191, _:K192, _:K193, _:N194, _:F197	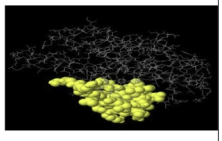
	_:V15, _:M19, _:R207	

(*continued on next page*)

Table 8 (*continued*)

		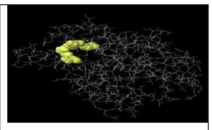
NS2B	_:V123, _:Y124, _:V125, _:K126, _:T127, _:G128, _:K129	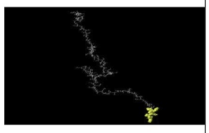
	_:P111, _:I112, _:A113, _:I114, _:P115, _:F116, _:A117, _:A118, _:G119, _:A120, _:W121, _:Y122	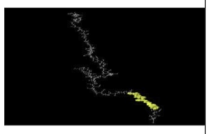
	_:S1, _:W2, _:P3, _:P4, _:S5, _:E6, _:V7, _:L8, _:T9, _:A10, _:V11, _:G12, _:L13, _:I14, _:C15, _:A16, _:L17, _:A18, _:G19, _:G20, _:F21	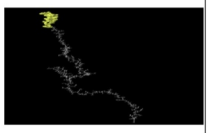
	_:E96, _:I97, _:I98, _:L99, _:K100, _:V101, _:V102, _:L103, _:M104	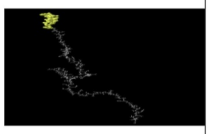
	_:D90, _:G91, _:P92, _:P93, _:M94, _:R95	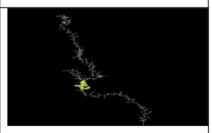
	_:A77, _:L78, _:D79, _:E80, _:S81, _:G82, _:D83, _:S85	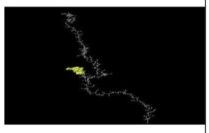
	_:D75, _:V87, _:E88	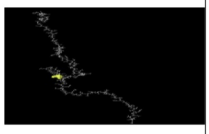
NS4A	_:V118, _:I120, _:P121, _:E122, _:P123, _:E124, _:K125	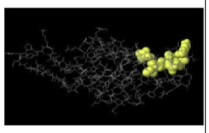
	_:A29, _:V30, _:L31, _:R33, _:A34, _:E35, _:T36, _:G37, _:S38, _:R39, _:P40, _:Y41, _:A43, _:A44, _:A45, _:A46, _:Q47	

(*continued on next page*)

Table 8 (*continued*)

		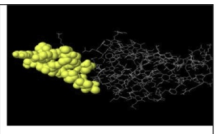
	_:G1, _:A2, _:L4, _:G5, _:M7, _:E8, _:A9, _:G11, _:T12, _:L13, _:P14, _:G15, _:H16, _:E19	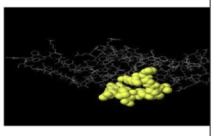
	_:L72, _:M73, _:N75, _:K76, _:G77, _:I78, _:G79, _:K80, _:M81	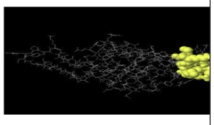
	_:E99, _:I100, _:E101, _:P102, _:A103, _:R104, _:C107	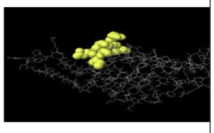
NS4B	_:L67, _:M68, _:A69, _:M70, _:A71, _:T72, _:Q73, _:A74, _:G75, _:V76, _:L77, _:F78, _:G79, _:M80, _:G81, _:K82, _:G83, _:M84, _:P85, _:F86	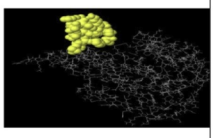
	_:P125, _:L127, _:Q128, _:A129, _:A130, _:A131, _:A132, _:R133, _:A134, _:A135, _:Q136, _:K137, _:T139, _:A140, _:A141, _:G142, _:I143, _:M144, _:K145, _:N146, _:P147, _:V148, _:V149, _:D150, _:G151	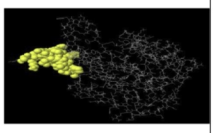
	_:A14, _:H15, _:L16, _:M17, _:G18, _:R19, _:R20, _:E21, _:E22, _:G23, _:A24, _:T25, _:M26, _:G27, _:F28, _:S29, _:M30, _:D31, _:I32, _:D33, _:L34, _:R35, _:P36, _:A37, _:S38, _:A39, _:I42, _:S102, _:Q103, _:L104, _:T105, _:A183, _:V184, _:R187, _:T188, _:A189, _:E208, _:G209, _:S210, _:P211, _:N212, _:K213, _:N216, _:S217, _:S218, _:A220, _:T221, _:S222, _:L223, _:C224, _:N225, _:F227, _:R228, _:G229, _:S230, _:Y231, _:L232, _:A233, _:G234, _:A235, _:S236, _:I238, _:Y239, _:T242, _:R243, _:A245, _:G246, _:L247, _:V248	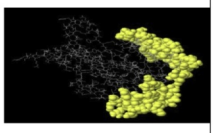
	_:N1, _:G4, _:E7, _:R8	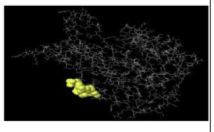
	_:W215, _:K249, _:R251	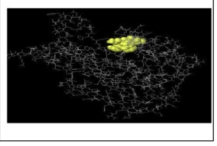

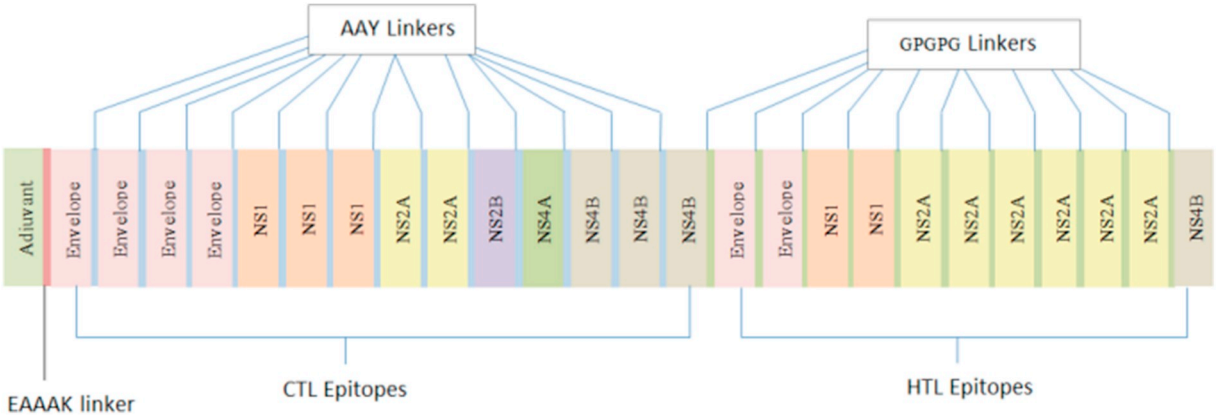

Fig. 2. Schematic diagram of MEBP vaccine construct: A 435 amino acid long MEBP vaccine sequence consisting an adjuvant (green) linked at N-terminal linked with a MEBP sequence with the help of EAAAK linker (pink).CTL epitopes are joined by AAY linkers (blue) while HTL epitoes are joined by GPGPG linkers (green).

Table 9
Conformational B cell epitopes in the final MEBP vaccine construct.

Conformational B cell Epitopes	3D Structure
_:L24, _:P25, _:K26, _:R43, _:K44	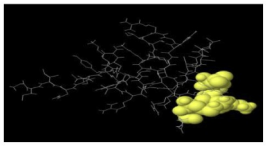
_:G1, _:I2, _:I3, _:N4, _:T5, _:L6, _:Q7, _:K8, _:Y9, _:R12	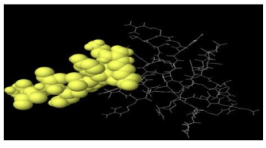
_:V20, _:L21, _:S22, _:C23, _:S34, _:T35, _:R36, _:G37, _:R38	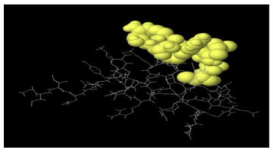

Table 10
Linear B cell epitopes in the final MEBP vaccine construct.

B cell Epitopes (Position)	Antigenicity	B cell Epitopes (Position)	Antigenicity
PGPGLAWLAIRAMAVP (397)	0.8	GDFSLAAYKMGFGMVT (163)	1.2
YRAAKTNNSFAAYIAL (98)	0.5	GPGALAWLAIRAMAVP (378)	0.9
FGPGPGSFIFRANWTP (335)	1.2	YGREAAHSDLAAYHSE (122)	0.6
PGSDLYYLTMNNKHWL (239)	0.6	FRANWTPRESMLGPGP (344)	1.4
GFSDLYYLTMNNKHWL (220)	0.9	VGPGPGSYFVRAAKTN (255)	0.6
GYFVRAAKTNNSFVVD (280)	0.5	LAALAAYGREAAHSDL (116)	0.7
EEQIGKCSTRGRKCCR (27)	1.3	GALVAAFKVRPALLVS (300)	1.0
WLAIRAMAVPRTGPGP (384)	0.6	CSTRGRKCCRRKKEAA (33)	1.3
VRAAKTNNSFVVGPGP (264)	0.7	YGLDFSDLYYAAYRLK(62)	1.2
IFRANWTPRESMLLGP (362)	1.0	PGLVAAFKVRPALLVS (319)	1.1
YSLAAYSTENSKMMLA(81)	0.6	KCCRRKKEAAAKSIQP (39)	0.6
AAAAYSAVLLRTAWGP (202)	0.7	AHYMYAAYYLIPGLQA (187)	0.7
RFAAYLLVAWRAGLAA (142)	0.5	AAYLDESGDFSLAAYK (156)	0.7
AKSIQPENLEYAAYGL (49)	1.4	YHSEELEIRFAAYLLV (134)	0.9
ENLEYAAYGLDFSDLY (55)	1.4	YKMGFGMVTLAAYILL (170)	0.9

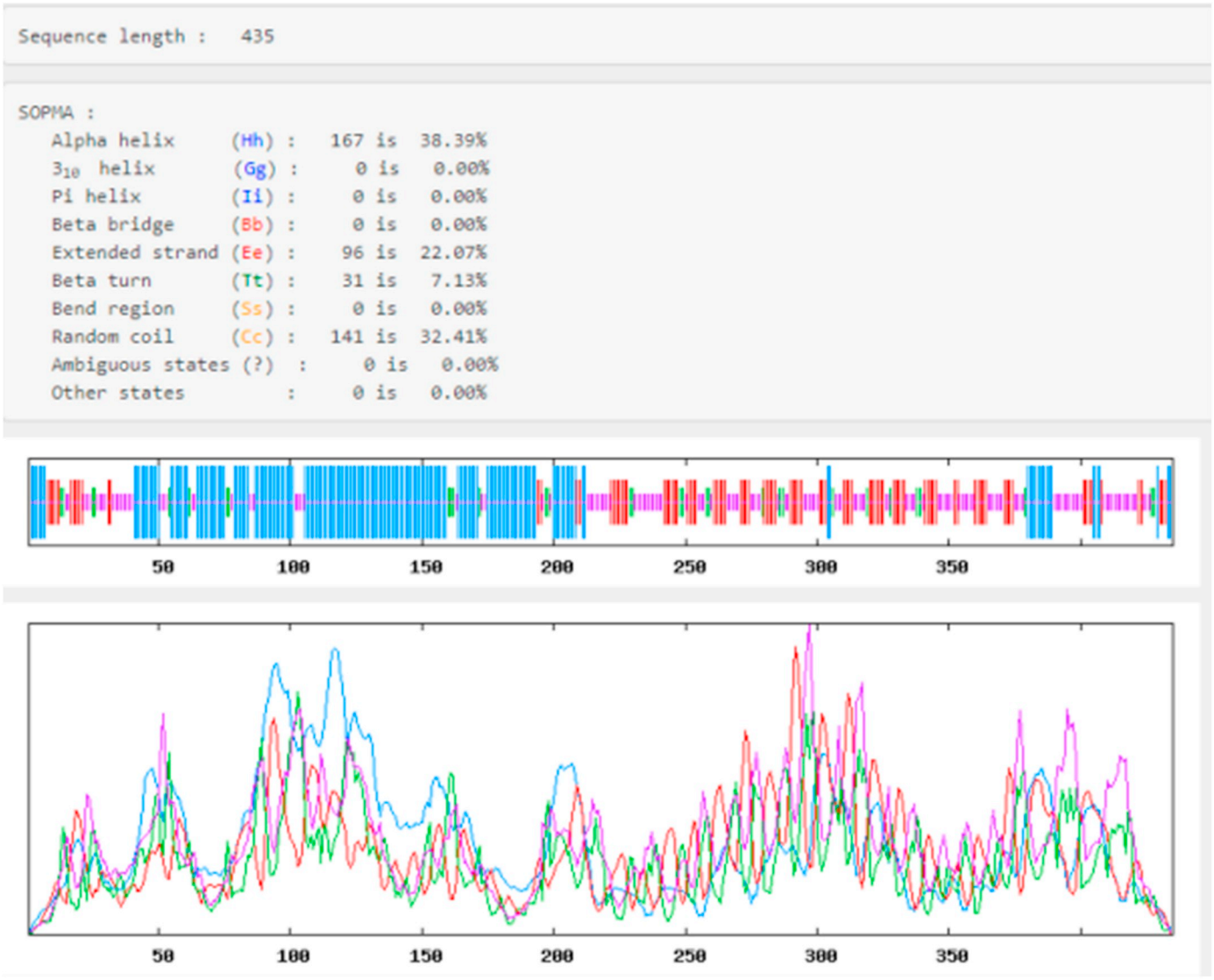

Fig. 3. Secondary structure properties of the vaccine. Two graphs are shown. First one is to visualize the prediction. The second contains curves for all predicted states.

Therefore, the current vaccine subunit is more immunogenic and effective against ZIKV infection.

MEBP vaccines are advantageous over the monovalent vaccine as it can elicit both cellular and humoral immunities (Amanna and Slifka, 2011). The prediction of B-cell and T-cell epitopes is an important step for the production of vaccines(Van Regenmortel, 1996). After prediction T-cell epitopes were screened for overlapping with B and IFN-γ epitopes. The selected epitopes were then analyzed for antigenicity prediction. For vaccine development, selected epitopes were merged by the assistance of AAY and GPGPG linkers and adjuvant was linked to the N-end of the vaccine. The incorporation of adjuvant in the designed multiepitope vaccines was meant to enhance immunogenicity and activated various mediators of adaptive and innate immunity (Perrie et al., 2008). Immunogenic adjuvant increases antibody production and helps in providing long-term protection (Ojha et al., 2019). Hence, a multi-epitope vaccine constructed cautiously utilizing such a methodology could turn into an integral asset to battle tumors and viral contaminations (Zhang, 2018). The results of the immunoinformatics approach recommend that the designed vaccine may undergo in vitro and in vivo experimental analyses to develop a potential vaccine against ZIKV infection.

5. Conclusion

ZIKV from being something obscure for a decade has now become a public problem of International concern. There is yet no vaccine or everlasting cure for the illness. Several antiviral drugs have underwent trials, but none displayed effective results against the infection. In current times, an effort was made to formulate a MEBP vaccine for ZIKV incorporating on the non-structural and structural proteins of the virus. Immunoinformatics and docking tools were utilized to develop a latent and secure MEBP vaccine that may trigger three types of immune reactions namely, cellular, humoral, and innate immune reactions. Stimulation of these immune responses might tend to control the virus infection. Also, this research enables the validation of this work by more comprehensive experimental approach. We assume that our predicted model of the vaccine will certainly demonstrate the positive effects to cure ZIKV infection.

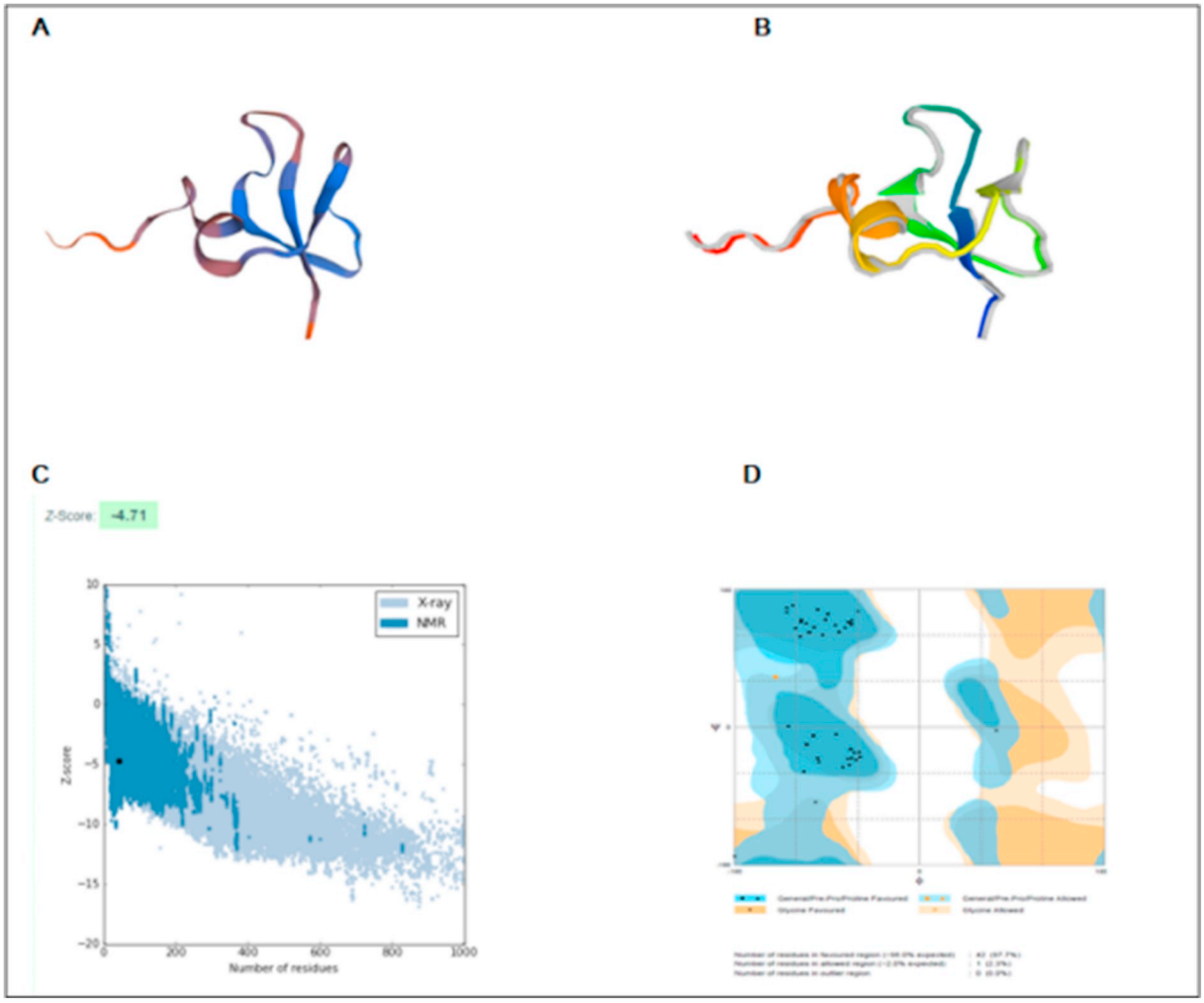

Fig. 4. Predicted 3D structure and validation of MEBP vaccine construct: (A) 3D structure of MEBP vaccine construct (B) Refined structure of MEBP vaccine construct. (C) PROSA validation of 3D MEBP construct (−4.71). (D) Ramachandran plot analysis of predicted structure.

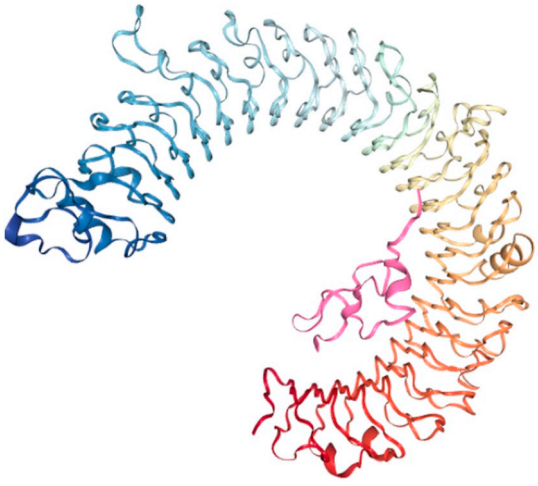

Fig. 5. MEBP Vaccine Construct-TLR3 docked complex. Pink color displayed the vaccine while rainbow color exhibited TLR-3. (For interpretation of the references to color in this figure legend, the reader is referred to the web version of this article.)

Declaration of Competing Interest

No financial and other conflict of interest related to this article.

Acknowledgements

The author would like to thank Government College University Faisalabad for providing facilities for this work.

References

Ahmad, B., Ashfaq, U.A., Rahman, M., Masoud, M.S., Yousaf, M.Z., 2019. Conserved B and T cell epitopes prediction of ebola virus glycoprotein for vaccine development: an immuno-informatics approach. Microb. Pathog. 132, 243–253.
Amanna, I.J., Slifka, M.K., 2011. Contributions of humoral and cellular immunity to vaccine-induced protection in humans. Virology 411, 206–215.
Arai, R., Ueda, H., Kitayama, A., Kamiya, N., Nagamune, T., 2001. Design of the linkers which effectively separate domains of a bifunctional fusion protein. Protein Eng. 14, 529–532.
Ashfaq, U.A., Ahmed, B., 2016. De novo structural modeling and conserved epitopes prediction of Zika virus envelop protein for vaccine development. Viral Immunol. 29, 436–443.
Barrett, A.D., 2016. Zika vaccine candidates progress through nonclinical development and enter clinical trials. NPJ Vaccines 1, 16023.
Benson, D.A., Karsch-Mizrachi, I., Lipman, D.J., Ostell, J., Sayers, E.W., 2008. GenBank. Nucleic Acids Res. 37, D26–D31.

Bergmann, C.C., Yao, Q., Ho, C.-K., Buckwold, S.L., 1996. Flanking residues alter antigenicity and immunogenicity of multi-unit CTL epitopes. J. Immunol. 157, 3242–3249.
Bjellqvist, B., Hughes, G.J., Pasquali, C., Paquet, N., Ravier, F., Sanchez, J.C., Frutiger, S., Hochstrasser, D., 1993. The focusing positions of polypeptides in immobilized pH gradients can be predicted from their amino acid sequences. Electrophoresis 14, 1023–1031.
Brennick, C.A., George, M.M., Corwin, W.L., Srivastava, P.K., Ebrahimi-Nik, H., 2017. Neoepitopes as cancer immunotherapy targets: key challenges and opportunities. Immunotherapy 9, 361–371.
Buathong, R., Hermann, L., Thaisomboonsuk, B., Rutvisuttinunt, W., Klungthong, C., Chinnawirotpisan, P., Manasatienkij, W., Nisalak, A., Fernandez, S., Yoon, I.-K., 2015. Detection of Zika virus infection in Thailand, 2012–2014. Am. J. Trop. Med Hyg. 93, 380–383.
Bui, H.-H., Sidney, J., Li, W., Fusseder, N., Sette, A., 2007. Development of an epitope conservancy analysis tool to facilitate the design of epitope-based diagnostics and vaccines. BMC Bioinformatics 8, 361.
Calvet, G., Aguiar, R.S., Melo, A.S., Sampaio, S.A., De Filippis, I., Fabri, A., Araujo, E.S., de Sequeira, P.C., de Mendonça, M.C., de Oliveira, L., 2016. Detection and sequencing of Zika virus from amniotic fluid of fetuses with microcephaly in Brazil: a case study. Lancet Infect. Dis. 16, 653–660.
Campos, G.S., Bandeira, A.C., Sardi, S.I., 2015. Zika virus outbreak, bahia, brazil. Emerg. Infect. Dis. 21, 1885.
Cao-Lormeau, V.-M., Roche, C., Teissier, A., Robin, E., Berry, A.-L., Mallet, H.-P., Sall, A.A., Musso, D., 2014. Zika virus, French polynesia, South Pacific, 2013. Emerg. Infect. Dis. 20, 1085.
Cardoso, C.W., Paploski, I.A., Kikuti, M., Rodrigues, M.S., Silva, M.M., Campos, G.S., Sardi, S.I., Kitron, U., Reis, M.G., Ribeiro, G.S., 2015. Outbreak of exanthematous illness associated with Zika, chikungunya, and dengue viruses, Salvador, Brazil. Emerg. Infect. Dis. 21, 2274.
Cauchemez, S., Besnard, M., Bompard, P., Dub, T., Guillemette-Artur, P., Eyrolle-Guignot, D., Salje, H., Van Kerkhove, M.D., Abadie, V., Garel, C., 2016. Association between Zika virus and microcephaly in French Polynesia, 2013–15: a retrospective study. Lancet 387, 2125–2132.
Chauhan, V., Rungta, T., Goyal, K., Singh, M.P., 2019. Designing a multi-epitope based vaccine to combat Kaposi sarcoma utilizing immunoinformatics approach. Sci. Rep. 9, 2517.
Davies, M.N., Flower, D.R., 2007. Harnessing bioinformatics to discover new vaccines. Drug Discov. Today 12, 389–395.
Davis, B.S., Chang, G.-J.J., Cropp, B., Roehrig, J.T., Martin, D.A., Mitchell, C.J., Bowen, R., Bunning, M.L., 2001. West Nile virus recombinant DNA vaccine protects mouse and horse from virus challenge and expresses in vitro a noninfectious recombinant antigen that can be used in enzyme-linked immunosorbent assays. J. Virol. 75, 4040–4047.
De Gregorio, E., Rappuoli, R., 2012. Vaccines for the future: learning from human immunology. Microb. Biotechnol. 5, 149–155.
Deléage, G., 2017. ALIGNSEC: viewing protein secondary structure predictions within large multiple sequence alignments. Bioinformatics 33 (24), 3991–3992.
Dhanda, S.K., Vir, P., Raghava, G.P., 2013. Designing of interferon-gamma inducing MHC class-II binders. Biol. Direct 8, 30.
Dimitrov, I., Flower, D.R., Doytchinova, I., 2013. AllerTOP-a server for in silico prediction of allergens. BMC Bioinforma S4 BioMed Central.
Doytchinova, I.A., Flower, D.R., 2007. VaxiJen: a server for prediction of protective antigens, tumour antigens and subunit vaccines. BMC Bioinforma. 8, 4.
Dubey, K.K., Luke, G.A., Knox, C., Kumar, P., Pletschke, B.I., Singh, P.K., Shukla, P., 2018. Vaccine and antibody production in plants: developments and computational tools. Brief. Funct. Genom. 17, 295–307.
Duffy, M.R., Chen, T.-H., Hancock, W.T., Powers, A.M., Kool, J.L., Lanciotti, R.S., Pretrick, M., Marfel, M., Holzbauer, S., Dubray, C., 2009. Zika virus outbreak on Yap Island, federated states of Micronesia. N. Engl. J. Med. 360, 2536–2543.
Fagbami, A., 1979. Zika virus infections in Nigeria: virological and seroepidemiological investigations in Oyo state. Epidemiol. Infect. 83, 213–219.
Faria, N.R., da Silva Azevedo, R.D.S., Kraemer, M.U., Souza, R., Cunha, M.S., Hill, S.C., Thézé, J., Bonsall, M.B., Bowden, T.A., Rissanen, I., 2016. Zika virus in the Americas: early epidemiological and genetic findings. Science 352, 345–349.
Faye, O., Freire, C.C., Iamarino, A., Faye, O., de Oliveira, J.V.C., Diallo, M., Zanotto, P.M., 2014. Molecular evolution of Zika virus during its emergence in the 20th century. PLoS Negl. Trop. Dis. 8, e2636.
Foy, B.D., Kobylinski, K.C., Foy, J.L.C., Blitvich, B.J., da Rosa, A.T., Haddow, A.D., Lanciotti, R.S., Tesh, R.B., 2011. Probable non–vector-borne transmission of Zika virus, Colorado, USA. Emerg. Infect. Dis. 17, 880.
Gillespie, G.M., Wills, M.R., Appay, V., O'Callaghan, C., Murphy, M., Smith, N., Sissons, P., Rowland-Jones, S., Bell, J.I., Moss, P.A., 2000. Functional heterogeneity and high frequencies of cytomegalovirus-specific CD8+ T lymphocytes in healthy seropositive donors. J. Virol. 74, 8140–8150.
Grote, A., Hiller, K., Scheer, M., Münch, R., Nörtemann, B., Hempel, D.C., Jahn, D., 2005. JCat: a novel tool to adapt codon usage of a target gene to its potential expression host. Nucleic Acids Res. 33, W526–W531.
He, R., Yang, X., Liu, C., Chen, X., Wang, L., Xiao, M., Ye, J., Wu, Y., Ye, L., 2018. Efficient control of chronic LCMV infection by a CD4 T cell epitope-based heterologous prime-boost vaccination in a murine model. Cell. Mol. Immunol. 15, 815.
Hennessey, M., Fischer, M., Staples, J.E., 2016. Zika virus spreads to new areas—region of the Americas, may 2015–January 2016. Am. J. Transplant. 16, 1031–1034.
Homan, J., Malone, R.W., Darnell, S.J., Bremel, R.D., 2016. Antibody mediated epitope mimicry in the pathogenesis of Zika virus related disease. bioRxiv. https://doi.org/10.1101/044834.
Ikram, A., Zaheer, T., Awan, F.M., Obaid, A., Naz, A., Hanif, R., Paracha, R.Z., Ali, A., Naveed, A.K., Janjua, H.A., 2018. Exploring NS3/4A, NS5A and NS5B proteins to design conserved subunit multi-epitope vaccine against HCV utilizing immunoinformatics approaches. Sci. Rep. 8, 16107.
Jensen, K.K., Andreatta, M., Marcatili, P., Buus, S., Greenbaum, J.A., Yan, Z., Sette, A., Peters, B., Nielsen, M., 2018. Improved methods for predicting peptide binding affinity to MHC class II molecules. Immunology 154, 394–406.
Jouannic, J.-M., Friszer, S., Leparc-Goffart, I., Garel, C., Eyrolle-Guignot, D., 2016. Zika virus infection in French Polynesia. Lancet 387, 1051–1052.
Kelley, L.A., Mezulis, S., Yates, C.M., Wass, M.N., Sternberg, M.J., 2015. The Phyre2 web portal for protein modeling, prediction and analysis. Nat. Protoc. 10, 845.
Khan, A., Junaid, M., Kaushik, A.C., Ali, A., Ali, S.S., Mehmood, A., Wei, D.-Q., 2018. Computational identification, characterization and validation of potential antigenic peptide vaccines from hrHPVs E6 proteins using immunoinformatics and computational systems biology approaches. PLoS One 13, e0196484.
Khatoon, N., Pandey, R.K., Prajapati, V.K., 2017. Exploring Leishmania secretory proteins to design B and T cell multi-epitope subunit vaccine using immunoinformatics approach. Sci. Rep. 7, 8285.
Kumar Pandey, R., Ojha, R., Mishra, A., Kumar Prajapati, V., 2018. Designing B-and T-cell multi-epitope based subunit vaccine using immunoinformatics approach to control Zika virus infection. J. Cell. Biochem. 119, 7631–7642.
Larsen, M.V., Lundegaard, C., Lamberth, K., Buus, S., Lund, O., Nielsen, M., 2007. Large-scale validation of methods for cytotoxic T-lymphocyte epitope prediction. BMC Bioinforma 8, 424.
Li, G., Poulsen, M., Fenyvuesvolgyi, C., Yashiroda, Y., Yoshida, M., Simard, J.M., Gallo, R.C., Zhao, R.Y., 2017. Characterization of cytopathic factors through genome-wide analysis of the Zika viral proteins in fission yeast. Proc. Natl. Acad. Sci. 114, E376–E385.
Lindenbach, B.D., Rice, C.M., 2003. Molecular biology of flaviviruses. Adv. Virus Res. 59, 23–62.
Livingston, B., Crimi, C., Newman, M., Higashimoto, Y., Appella, E., Sidney, J., Sette, A., 2002. A rational strategy to design multiepitope immunogens based on multiple Th lymphocyte epitopes. J. Immunol. 168, 5499–5506.
Lovell, S.C., Davis, I.W., Arendall III, W.B., De Bakker, P.I., Word, J.M., Prisant, M.G., Richardson, J.S., Richardson, D.C., 2003. Structure validation by Cα geometry: ϕ, ψ and Cβ deviation. Proteins: Structure, Function, and Bioinformatics 50, 437–450.
Lu, C., Meng, S., Jin, Y., Zhang, W., Li, Z., Wang, F., Wang-Johanning, F., Wei, Y., Liu, H., Tu, H., 2017. A novel multi-epitope vaccine from MMSA-1 and DKK 1 for multiple myeloma immunotherapy. Br. J. Haematol. 178, 413–426.
Macnamara, F., 1954. Zika virus: a report on three cases of human infection during an epidemic of jaundice in Nigeria. Trans. R. Soc. Trop. Med. Hyg. 48, 139–145.
Malet, H., Massé, N., Selisko, B., Romette, J.-L., Alvarez, K., Guillemot, J.C., Tolou, H., Yap, T.L., Vasudevan, S.G., Lescar, J., 2008. The flavivirus polymerase as a target for drug discovery. Antivir. Res. 80, 23–35.
Mallet, H.-P., Vial, A.-L., Musso, D., 2016. Bilan de l'épidémie à virus Zika survenue en Polynésie française entre octobre 2013 et mars 2014. De la description de l'épidémie aux connaissances acquises après l'évènement. Bull Epidémiol Hebd 20–21, 367–373.
Mirza, M.U., Rafique, S., Ali, A., Munir, M., Ikram, N., Manan, A., Salo-Ahen, O.M., Idrees, M., 2016. Towards peptide vaccines against Zika virus: Immunoinformatics combined with molecular dynamics simulations to predict antigenic epitopes of Zika viral proteins. Sci. Rep. 6, 37313.
Mohan, T., Sharma, C., Bhat, A.A., Rao, D., 2013. Modulation of HIV peptide antigen specific cellular immune response by synthetic α-and β-defensin peptides. Vaccine 31, 1707–1716.
Mohan, T., Mitra, D., Rao, D., 2014. Nasal delivery of PLG microparticle encapsulated defensin peptides adjuvanted gp41 antigen confers strong and long-lasting immunoprotective response against HIV-1. Immunol. Res. 58, 139–153.
Monath, T.P., Guirakhoo, F., Nichols, R., Yoksan, S., Schrader, R., Murphy, C., Blum, P., Woodward, S., McCarthy, K., Mathis, D., 2003. Chimeric live, attenuated vaccine against Japanese encephalitis (ChimeriVax-JE): phase 2 clinical trials for safety and immunogenicity, effect of vaccine dose and schedule, and memory response to challenge with inactivated Japanese encephalitis antigen. J. Infect. Dis. 188, 1213–1230.
Moore, D.á., Causey, O., Carey, D., Reddy, S., Cooke, A., Akinkugbe, F., David-West, T., Kemp, G., 1975. Arthropod-borne viral infections of man in Nigeria, 1964–1970. Ann. Trop. Med. Parasitol. 69, 49–64.
Musso, D., Roche, C., Robin, E., Nhan, T., Teissier, A., Cao-Lormeau, V.-M., 2015. Potential sexual transmission of Zika virus. Emerg. Infect. Dis. 21, 359.
Nezafat, N., Karimi, Z., Eslami, M., Mohkam, M., Zandian, S., Ghasemi, Y., 2016. Designing an efficient multi-epitope peptide vaccine against Vibrio cholerae via combined immunoinformatics and protein interaction based approaches. Comput. Biol. Chem. 62, 82–95.
Nowakowski, T.J., Pollen, A.A., Di Lullo, E., Sandoval-Espinosa, C., Bershteyn, M., Kriegstein, A.R., 2016. Expression analysis highlights AXL as a candidate Zika virus entry receptor in neural stem cells. Cell Stem Cell 18, 591–596.
Ojha, R., Pareek, A., Pandey, R.K., Prusty, D., Prajapati, V.K., 2019. Strategic development of a next-generation multi-epitope vaccine to prevent Nipah virus zoonotic infection. ACS Omega 4, 13069–13079.
Olson, J., Ksiazek, T., 1981. Zika virus, a cause of fever in Central Java, Indonesia. Trans. R. Soc. Trop. Med. Hyg. 75, 389–393.
Pandey, R.K., Narula, A., Naskar, M., Srivastava, S., Verma, P., Malik, R., Shah, P., Prajapati, V.K., 2017. Exploring dual inhibitory role of febrifugine analogues against Plasmodium utilizing structure-based virtual screening and molecular dynamic simulation. J. Biomol. Struct. Dyn. 35, 791–804.
Pandey, R.K., Bhatt, T.K., Prajapati, V.K., 2018. Novel immunoinformatics approaches to design multi-epitope subunit vaccine for malaria by investigating anopheles salivary

protein. Sci. Rep. 8, 1125.
Patronov, A., Doytchinova, I., 2013. T-cell epitope vaccine design by immunoinformatics. Open Biol. 3, 120139.
Peng, J., Xu, J., 2011. RaptorX: exploiting structure information for protein alignment by statistical inference. Proteins: Structure, Function, and Bioinformatics 79, 161–171.
Perera, R., Khaliq, M., Kuhn, R.J., 2008. Closing the door on flaviviruses: entry as a target for antiviral drug design. Antivir. Res. 80, 11–22.
Perrie, Y., Mohammed, A.R., Kirby, D.J., McNeil, S.E., Bramwell, V.W., 2008. Vaccine adjuvant systems: enhancing the efficacy of sub-unit protein antigens. Int. J. Pharm. 364, 272–280.
Prevention, E.C.f.D., Control, 2014. Rapid risk Assessment: Zika Virus Infection Outbreak, French Polynesia: 14 February 2014. European Centre for Disease Prevention and Control Stockhom.
Putnak, R., Barvir, D.A., Burrous, J.M., Dubois, D.R., D'Andrea, V.M., Hoke, C.H., Sadoff, J.C., Eckels, K.H., 1996. Development of a purified, inactivated, dengue-2 virus vaccine prototype in Vero cells: immunogenicity and protection in mice and rhesus monkeys. J. Infect. Dis. 174, 1176–1184.
Saha, S., Raghava, G., 2006. Prediction of continuous B-cell epitopes in an antigen using recurrent neural network. Proteins: Structure, Function, and Bioinformatics 65, 40–48.
Schuler-Faccini, L., 2016. Possible association between Zika virus infection and microcephaly—Brazil, 2015. MMWR Morb. Mortal. Wkly Rep. 65.
Shin, W.-H., Lee, G.R., Heo, L., Lee, H., Seok, C., 2014. Prediction of protein structure and interaction by GALAXY protein modeling programs. Bio Design 2, 1–11.
Sirohi, D., Kuhn, R.J., 2017. Zika virus structure, maturation, and receptors. J. Infect. Dis. 216, S935–S944.
Stasyk, T., Huber, L.A., 2016. Spatio-temporal parameters of endosomal signaling in Cancer: implications for new treatment options. J. Cell. Biochem. 117, 836–843.
Tahir ul Qamar, M., Bari, A., Adeel, M.M., Maryam, A., Ashfaq, U.A., Du, X., Muneer, I., Ahmad, H.I., Wang, J., 2018. Peptide vaccine against chikungunya virus: immunoinformatics combined with molecular docking approach. J. Transl. Med. 16, 298.
Van Regenmortel, M.H., 1996. Mapping epitope structure and activity: from one-dimensional prediction to four-dimensional description of antigenic specificity. Methods 9, 465–472.
Victora, C.G., Schuler-Faccini, L., Matijasevich, A., Ribeiro, E., Pessoa, A., Barros, F.C., 2016. Microcephaly in Brazil: how to interpret reported numbers? Lancet 387, 621–624.
Walker, J.M., 2005. The Proteomics Protocols Handbook. Springer.
Wang, P., Sidney, J., Kim, Y., Sette, A., Lund, O., Nielsen, M., Peters, B., 2010. Peptide binding predictions for HLA DR, DP and DQ molecules. BMC Bioinforma. 11, 568.
Waterhouse, A., Bertoni, M., Bienert, S., Studer, G., Tauriello, G., Gumienny, R., Heer, F.T., de Beer, T.A.P., Rempfer, C., Bordoli, L., 2018. SWISS-MODEL: homology modelling of protein structures and complexes. Nucleic Acids Res. 46, W296–W303.
WHO, 2015. Zika virus outbreaks in the Americas. Wkly Epidemiol. Rec. 90, 609–610.
Wiederstein, M., Sippl, M.J., 2007. ProSA-web: interactive web service for the recognition of errors in three-dimensional structures of proteins. Nucleic Acids Res. 35, W407–W410.
Yan, Y., Zhang, D., Zhou, P., Li, B., Huang, S.-Y., 2017. HDOCK: a web server for protein–protein and protein–DNA/RNA docking based on a hybrid strategy. Nucleic Acids Res. 45, W365–W373.
Yang, X., Yu, X., 2009. An introduction to epitope prediction methods and software. Rev. Med. Virol. 19, 77–96.
Zanluca, C., Melo, V.C.A., Mosimann, A.L.P., Santos, G.I.V., Santos, C.N.D., Luz, K., 2015. First report of autochthonous transmission of Zika virus in Brazil. Mem. Inst. Oswaldo Cruz 110, 569–572.
Zhang, L., 2018. Multi-epitope vaccines: a promising strategy against tumors and viral infections. Cell. Mol. Immunol. 15, 182.